J Toxicol Pathol 2022; 35: 37–44

Original Article

Effects of testosterone on rat placental development

Satoshi Furukawa[1*], Naho Tsuji[1], Seigo Hayashi[1], Yusuke Kuroda[1], Masayuki Kimura[1], Chisato Hayakawa[1], Kazuya Takeuchi[1], and Akihiko Sugiyama[2]

[1] Biological Research Laboratories, Nissan Chemical Corporation, 1470 Shiraoka, Shiraoka-shi, Saitama 349-0294, Japan
[2] Veterinary Clinical Pathology, Faculty of Veterinary Medicine, Okayama University of Science, 1-3 Ikoinooka, Imabari-shi, Ehime 794-8555, Japan

Abstract: We investigated the morphological effects of testosterone on placental development in a rat model of polycystic ovarian syndrome (PCOS). Testosterone propionate (TP), which was subcutaneously administered to pregnant rats with 5 mg/animal from gestation day (GD) 14 to GD 18, induced a maternal weight reduction without mortality or clinical signs from GD 19 onwards. A decrease in fetal and placental weight, an increase in intrauterine growth retardation (IUGR) rates, and histological changes in the placenta were observed on GD 21 but not on GD15 or 17. Histopathologically, on GD 21, the trophoblast septa thickened, and the maternal sinusoids were narrowed in the labyrinth zone, resulting in a small placenta. Additionally, the placental weight, thickness, and histological morphology in the labyrinth zone on GD 21 in the TP-treated group were nearly identical to those on GD 17 in the control and TP-treated groups. Therefore, it was assumed that the testosterone-induced small placenta was induced in association with the developmental inhibition of the fetal part of the placentas from GD 17 onwards. (DOI: 10.1293/tox.2021-0035; J Toxicol Pathol 2022; 35: 37–44)

Key words: IUGR, labyrinth zone, PCOS, small placenta, trophoblast

Introduction

Elevated testosterone levels are involved in pregnancy-related complications, such as preeclampsia[1] and polycystic ovarian syndrome (PCOS)[2] in humans. PCOS is an endocrine disorder in women, and its common features are abnormal ovulation, hyperandrogenemia, and polycystic ovaries[3, 4]. PCOS also induces an increased risk of pregnancy and neonatal complications, intrauterine growth restriction (IUGR), and a low body weight of offspring in humans[5]. In rats, high-dose testosterone administration can induce toxic reproductive effects, such as reduced litter size, low body weight of offspring, and decreased reproductive capacity for dams, including delayed parturition and increased resorption[6]. Moreover, testosterone induces IUGR and a decreased placental weight[7]. It is thought that elevated maternal testosterone has adverse effects on fetal development, mediated by placental hypofunction without affecting fetal testosterone levels[8, 9]. However, there have been no reports to date that describe the detailed sequential histopathological changes in placentas during the gestation period in testosterone-exposed pregnant rats. In the present study, we subcutaneously administrated testosterone to the pregnant rats from gestation days (GD) 14 to 18 and performed a histopathological examination of their placentas on GDs 15, 17, and 21 in order to elucidate the morphological effects of testosterone on placental development in the testosterone-induced rat model of PCOS.

Received: 28 May 2021, Accepted: 23 August 2021
Published online in J-STAGE: 16 September 2021
*Corresponding author: S Furukawa
(e-mail: furukawa@nissanchem.co.jp)

Materials and Methods

Animals

Pregnant (GD 6), specific-pathogen-free Wistar Hannover rats (Japan Laboratory Animals, Inc., Hanno, Japan) were purchased at approximately 11–12 wk of age. GD 0 was designated as the day when the presence of a vaginal plug was identified. The animals were single-housed in plastic cages on softwood chip bedding in an air-conditioned room (22 ± 2 °C; 55 ± 10% humidity; 12 h/d light cycle). Food (CRF-1: Oriental Yeast Co., Ltd., Tokyo, Japan) and water were available *ad libitum*.

Experimental design

In total, 24 pregnant rats were randomly allocated into two groups of 12 rats each (Table 1). Testosterone propionate (TP) (Sigma-Aldrich, St. Louis, MO, USA), suspended in olive oil, was administered subcutaneously to one group at a dose of 5 mg/animal at a volume of 0.1 mL/body weight

from GD 14 to GD 18. This 5 mg/animal TP or free testosterone dose has previously been reported to induce reproductive toxicity in the testosterone-induced rat model of PCOS[6, 7]. The animals in the control group were dosed similarly with olive oil alone. All of the treatments were administered between 9 and 11 a.m. Maternal body weight was recorded on GDs 6, 8, 10, 13, 15, 17, 19, 20, and 21. The dams (n=4/each time point/group) were sampled on GDs 15, 17, and 21. The dams were euthanized via exsanguination under isoflurane anesthesia and necropsied. All of the fetuses were removed from their placentas. A third of the placentas were separated between the basal zone and the decidua basalis, and removed from the uterus wall. The fetuses and removed placentas were weighed, and their individual fetal-placental weight ratios were calculated. The fetuses were macroscopically examined for external malformations on GD 21. According to criteria for IUGR evaluation, the fetuses were defined as having IUGR if their weights were -2 standard deviations (SD) from the mean for fetuses in the control group on each GD[10], which, in the present study, was <0.24 g on GD 15, <0.70 g on GD 17, and <5.21 g on GD 21. The IUGR rate (i.e., the actual number of fetuses exhibiting IUGR as a percentage of the total number of fetuses) was calculated. All of the fetal and placental samples were fixed in 10% neutral buffered formalin. This study was conducted according to the Guidelines for Animal Experimentation, Biological Research Laboratory, Nissan Chemical Corporation, and the Statement about sedation, anesthesia, and euthanasia in a rodent fetus and newborn (2015) in the Japanese College of Laboratory Animal Medicine.

Histopathological examination

Four placentas randomly selected for each dam were embedded in one paraffin block, and 4-µm thick sections were routinely stained with hematoxylin and eosin (HE) stain for histopathological examination on GDs 15, 17, and 21. All of these placentas were subjected to phospho-histone H3 (Ser10) (Cell Signaling Technology, Boston, MA, USA) immunohistochemical staining, Factor VIII related antigen (DAKO, Tokyo, Japan) immunohistochemical staining, and *in situ* TdT-mediated dUTP nick end labeling (TUNEL; *In Situ* Cell Death Detection Kit, POD, Roche Applied Science, Penzberg, Germany)[11]. The thicknesses of the labyrinth zone, basal zone, decidua basalis, and metrial gland close to the central portion of the placentas were measured once per one placenta using an image analyzer (WinROOF, Mitani Co., Tokyo, Japan). With the aid of the image analyzer, the number of cells in the trophoblastic septa at the base region of the labyrinth zone were counted in five sections per one placenta in the HE-stained slides using light microscopy with a 40× objective. The numbers of phospho-histone H3-positive cells and TUNEL-positive cells in the labyrinth zone, basal zone, metrial gland, and yolk sac were counted in 20 sections per one placenta across the entire cross-section using light microscopy with a 40× objective. The number of spiral arteries surrounded by the interstitial trophoblasts and/or uNK-cells and the number of these with the endovascular trophoblast invasion were counted in the decidua basalis and metrial gland in the HE-stained slides on GDs 15 and 17. The above aforementioned histopathological analyses were performed on all prepared placenta specimens, and the mean values of each analysis for each litter were calculated.

Statistical analysis

The means and SD of the individual litter values were calculated (Pharmaco Basic, Scientist Press Co. Ltd., Tokyo, Japan). For comparisons between both groups, either the Student's t-test for homoscedastic data or the Aspin-Welch's t-test for non-homoscedastic data was performed after the F-test. The Fisher's exact test was performed for the incidence of IUGR. The levels of significance were set at $p<0.05$ and <0.01.

Results

Effects on dams

The body weight gain (%) of dams in the TP-treated group (based on the body weight on GD 6 as 100%) tended to decrease from GD 19 onwards, compared with the control group (Fig. 1). No mortality or clinical signs were observed in any dams in either group during the experimental period.

Table 1. Effects of Testosterone on Placentas and Fetuses

Autopsy	Group	No. of dams	Mean No. of live fetuses[a)]	Fetal mortality (%)[a)]	Fetus weight (g)[a)]	Placenta weight (g)[a)]	Fetus / Placenta (g/g)[a)]	IUGR rate (%)
GD15	Control	4	10.3 ± 2.2	9.1 ± 18.2	0.27 ± 0.02	0.23 ± 0.03	1.33 ± 0.24	7.3
	Testosterone	4	10.3 ± 1.7	2.3 ± 4.5	0.28 ± 0.01	0.20 ± 0.03	1.27 ± 0.17	0.0
GD17	Control	4	9.8 ± 1.3	5.1 ± 5.9	0.82 ± 0.06	0.34 ± 0.04	2.44 ± 0.19	5.1
	Testosterone	4	10.5 ± 1.3	2.3 ± 4.5	0.82 ± 0.03	0.33 ± 0.02	2.53 ± 0.26	5.0
GD21	Control	4	11.3 ± 1.3	2.1 ± 4.2	5.80 ± 0.20	0.53 ± 0.04	10.89 ± 0.59	4.9
	Testosterone	4	11.5 ± 1.7	6.5 ± 8.6	3.53 ± 0.37**	0.39 ± 0.02**	8.76 ± 1.05*	100.0##

Mean ± SD.

a) Mean of individual litter values.

*, ** Significantly different from control at $p<0.05$, <0.01, respectively (Student's t-test).

Significantly different from control at $p<0.01$ (Fisher exact test).

Effects on embryos/fetuses and placentas

The effects of testosterone on fetuses and placentas are shown in Table 1. There were no effects of testosterone on the number of live fetuses or fetal mortality rate during the experimental period, nor on fetal weight, placental weight, fetal-placental weight ratio, or IUGR rates on GDs 15 and 17. On GD 21, fetal weight, placental weight, and fetal-placental weight ratio decreased, and IUGR rates increased in the TP-treated group, compared with the control group. Upon fetal external examination, increased anogenital distance in the female fetuses on GD 21 was observed in the TP-treated group (data not shown).

Histopathological observations

On GDs 15 and 17, there were no changes in the thickness of any part of the placenta (Fig. 2), the number of cells in the trophoblastic septa at the base region of the labyrinth zone (Fig. 3), or the histological morphology of the labyrinth zone (Fig. 4a) and basal zone in the TP-treated group. Although there were no differences in the total number of spiral arteries surrounded by the interstitial trophoblasts and/or uNK-cells in the decidua basalis and metrial gland in both groups, their number with the endovascular trophoblast invasion increased on GD 15 in the TP-treated group (Figs. 4b, 4c, and 5).

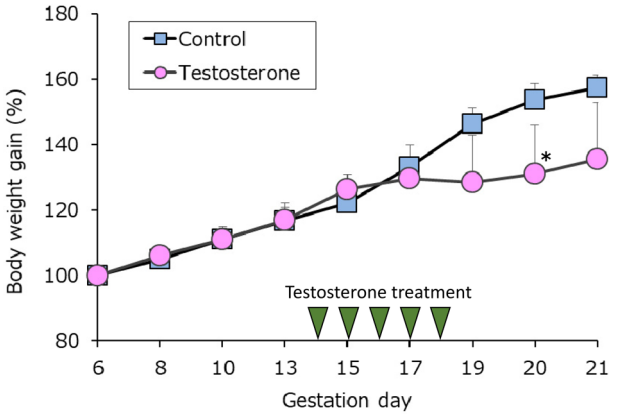

Fig. 1. Maternal body weight changes.
*Significantly different from control at p<0.05 (Student's t-test).
Standard deviation (SD): Error bar.

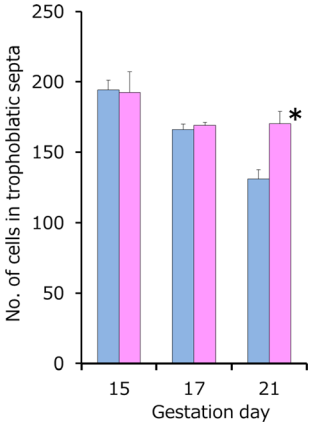

Fig. 3. Number of cells in trophoblastic septa at the base region of the labyrinth zone.
Each value represents mean ± standard deviation.
Blue bar, Control; Pink bar, Testosterone.
* Significantly different from control at p<0.05 (Student's t-test).

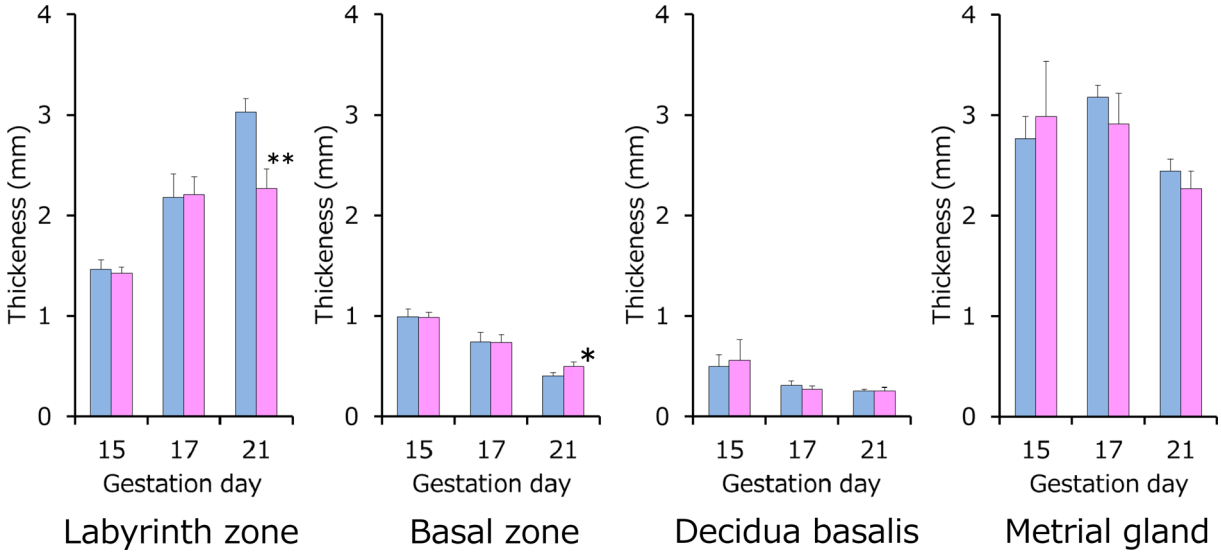

Fig. 2. Thickness of labyrinth zone, basal zone, decidua basalis, and metrial gland.
Blue bar, Control; Pink bar, Testosterone.
Each value represents mean ± standard deviation.
*, ** Significantly different from control at p<0.05, <0.01, respectively (Student's t-test).

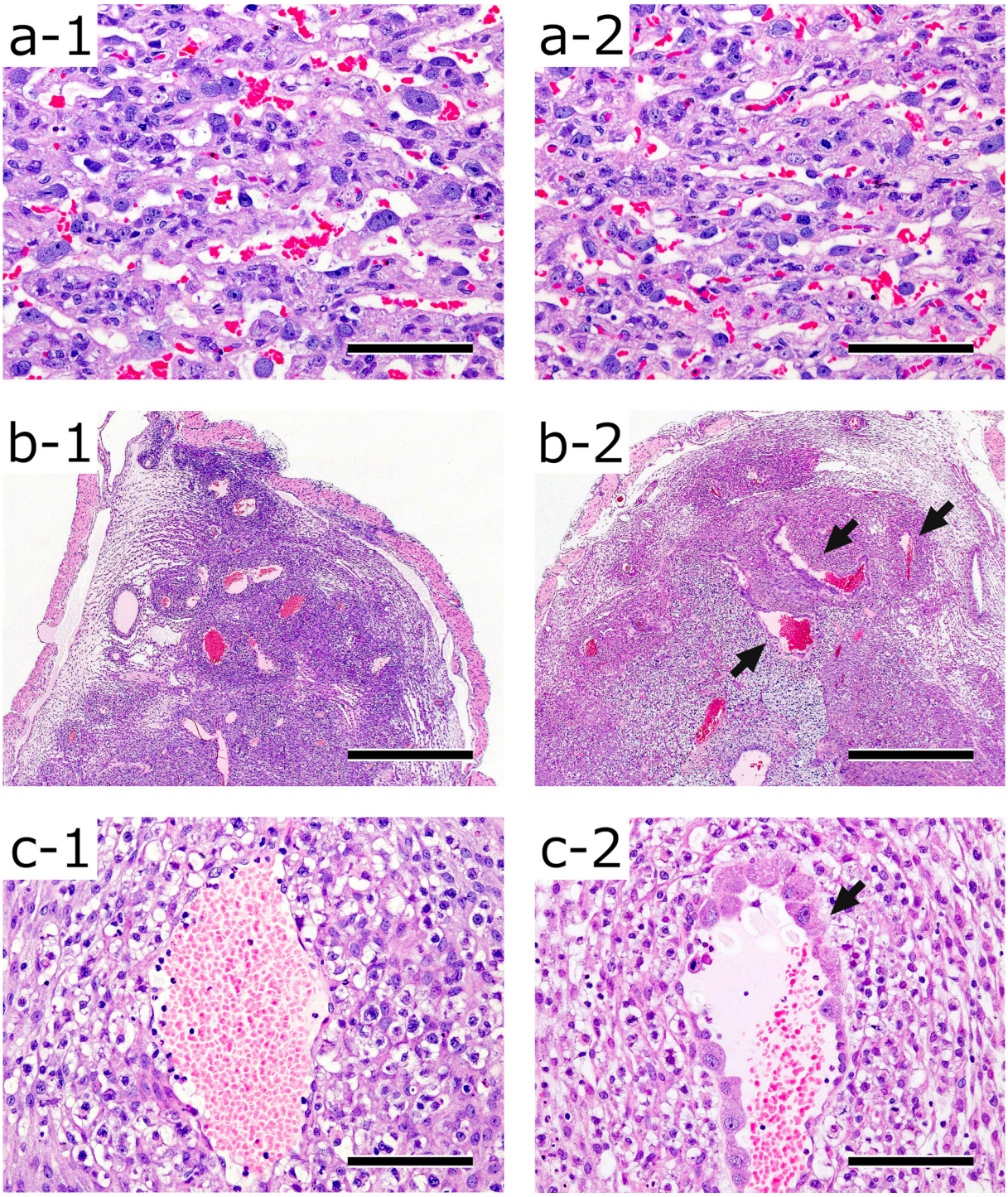

Fig. 4. Histopathological placenta findings.
a. Labyrinth zone on gestation day (GD) 15.
1. Control group. 2. Testosterone propionate (TP)-treated group. No differences in histological morphology between control and TP-treated groups. Bar, 110 μm. Hematoxylin and eosin (HE) stain.
b. Metrial gland on GD 15.
1. Control group. 2. TP-treated group. Increased number of spiral arteries surrounded by interstitial trophoblasts and/or uNK-cells with endovascular trophoblast invasion (→). Bar, 1,100 μm. HE stain.
c. Metrial gland on GD 15 (high magnification).
1. Control group. 2. TP-treated group. Endovascular trophoblast invasion into spiral artery (→). Bar, 110 μm. HE stain.

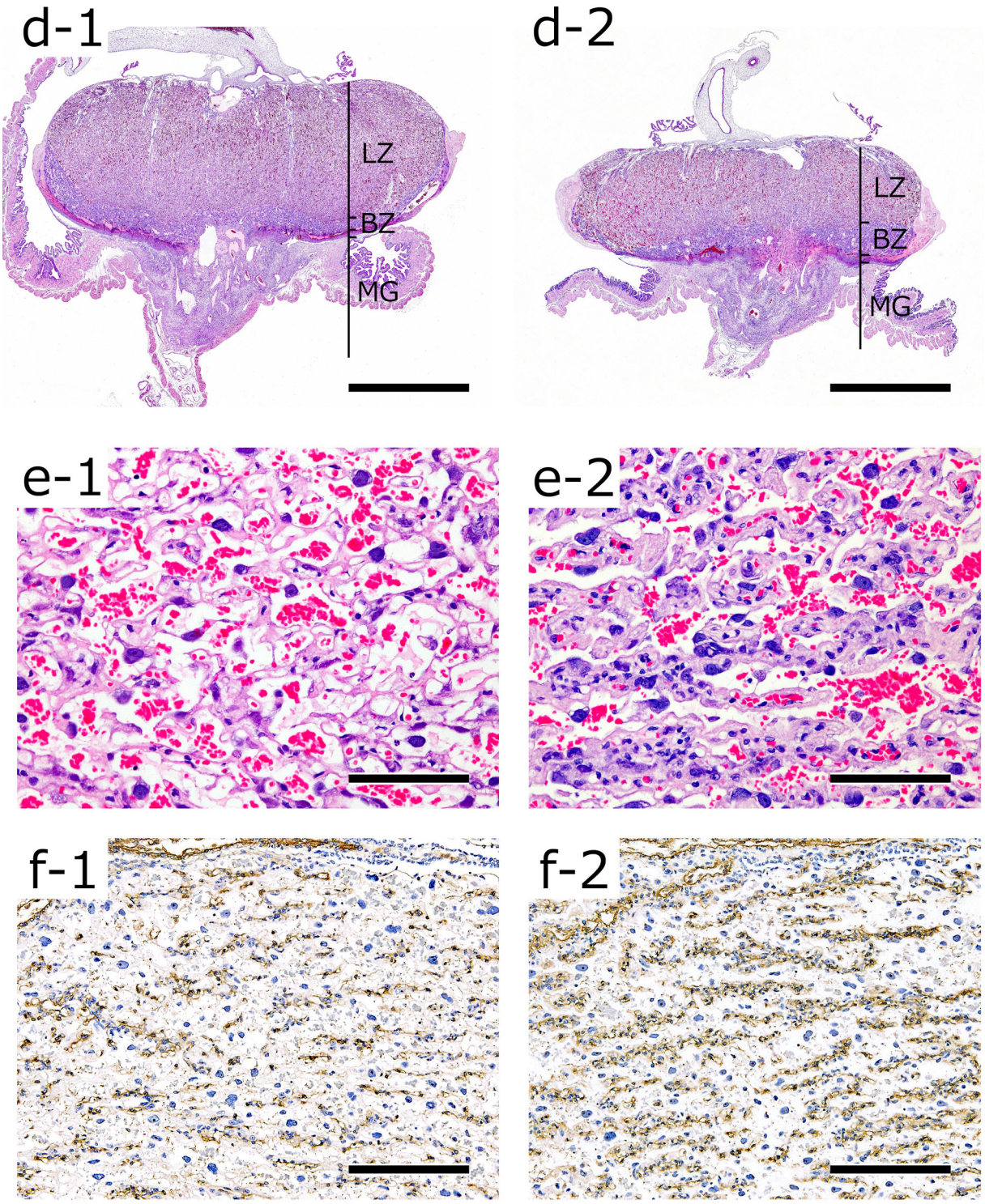

Fig. 4. Continued.
d. Loupe image of placenta on GD 21.
1. Control group. 2. TP-treated group. Thinning of labyrinth zone and slight thickening of basal zone. Bar, 3,160 μm. HE stain.
e. Histological changes in labyrinth zone on GD 21.
1. Control group. 2. TP-treated group. Thickening of trophoblast septa and narrowing of maternal sinusoids. Bar, 110 μm. HE stain.
f. Histological changes in labyrinth zone on GD 21.
1. Control group. 2. TP-treated group. Increased Factor VIII-positive endothelial cell density in fetal capillaries. Bar, 220 μm. Factor VIII immunohistochemical stain.
LZ: labyrinth zone; BZ: basal zone; MG: metrial gland.

On GD 21, the labyrinth zone thinned, and the basal zone slightly thickened in the TP-treated group, resulting in a small placenta (Figs. 2 and 4d). The trophoblast septa thickened and the maternal sinusoids narrowed in the labyrinth zone (Fig. 4e). Corresponding to the histological changes, Factor VIII-positive endothelial cell density in fetal capillaries in the labyrinth zone increased in the TP-treated group (Fig. 4f). However, the histological morphology in the labyrinth zone on GD 21 in the TP-treated group was nearly identical to that on GD 17 in both groups. In addition, the number of cells in the trophoblastic septa at the base region of the labyrinth zone on GD 21 in the TP-treated group was greater than that on GD 21 in the control group, but it was almost the same as that on GD 17 in both groups (Fig. 3).

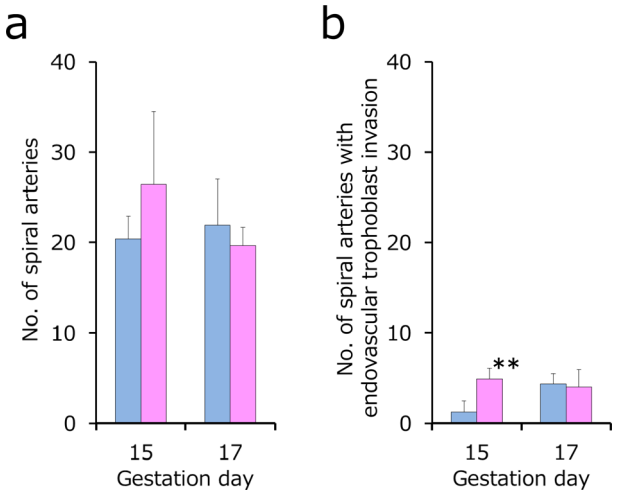

Fig. 5. Number of spiral arteries in decidua basalis and metrial gland.
a. Total number of spiral arteries. b. Number of spiral arteries with endovascular trophoblast invasion.
Blue bar, Control; Pink bar, Testosterone.
Each value represents mean ± standard deviation.

During the experimental period, there were no changes in the histological morphology of the yolk sac or the number of TUNEL-positive cells and phospho-histone H3-positive cells in any part of the placenta (Table 2).

Discussion

Elevated maternal testosterone induces a reduction in placental size and weight in pregnant women with PCOS[12, 13] and in the testosterone-induced rat model of PCOS[7, 8]. It is considered that reduced trophoblast invasion[14], testosterone-induced autophagy[14], or advanced placental differentiation[15] likely contribute to testosterone-induced alterations in placental weight and morphology. In addition, since testosterone enhances apoptotic damages in cultured human vascular endothelial cells[16], the testosterone-induced small placenta is assumed to have had developed due to increased apoptosis or decreased cell proliferation[17]. However, these morphological changes have not been confirmed in the testosterone-induced rat model of PCOS. In the present study, we examined sequential histopathological changes in rat placentas exposed to testosterone from GD 14 to GD 18. The placentas on GD 21 showed a thickening of trophoblast septa and a narrowing of maternal sinusoids in the labyrinth zone, with a reduced placental size and weight. These histopathological findings in the labyrinth zone on GD 21 were consistent with the testosterone-induced changes in the previous report on the rat model[7]. In contrast, there were no obvious changes in the placental weight or histological morphology of the placentas on GDs 15 and 17. The placental weight and histological morphology in the labyrinth zone on GD 21 in the TP-treated group were nearly identical to those in the normal developing placenta on GD 17. Furthermore, the basal zone on GD 21 thickened in the TP-treated group. During normal rat placental development, the basal zone becomes thinned due to regression from GD 15 onwards, and the labyrinth zone outgrows due to more blood content as pregnancy progresses, as a consequence of dilatation of

Table 2. Cell Proliferation and Apoptosis in Placenta

	Autopsy	Group	Labyrinth zone	Basal zone	Metrial gland	Yolk sac
No. of Histone H3 positive cells[1)]	GD 15	Control	43.9 ± 3.0	0.1 ± 0.1	10.6 ± 3.6	50.7 ± 14.2
		Testosterone	44.9 ± 3.8	0.3 ± 0.2	11.1 ± 3.2	48.3 ± 5.1
	GD 17	Control	15.0 ± 1.5	0.1 ± 0.1	8.0 ± 2.6	38.7 ± 5.3
		Testosterone	14.2 ± 2.2	0.0 ± 0.0	5.8 ± 1.0	40.0 ± 7.9
	GD 21	Control	0.0 ± 0.0	0.0 ± 0.0	0.8 ± 0.6	0.0 ± 0.0
		Testosterone	0.1 ± 0.2	0.0 ± 0.0	0.6 ± 0.7	0.2 ± 0.3
No. of TUNEL positive cells[1)]	GD 15	Control	1.2 ± 0.7	0.1 ± 0.1	44.9 ± 6.1	0.0 ± 0.0
		Testosterone	2.6 ± 1.5	0.0 ± 0.0	46.1 ± 11.6	0.0 ± 0.0
	GD 17	Control	1.2 ± 0.5	0.3 ± 0.4	53.8 ± 13.9	0.1 ± 0.1
		Testosterone	1.3 ± 0.8	0.1 ± 0.1	56.1 ± 9.4	0.0 ± 0.0
	GD 21	Control	0.4 ± 0.1	29.2 ± 13.1	40.3 ± 10.2	0.0 ± 0.0
		Testosterone	0.3 ± 0.2	25.1 ± 8.1	47.9 ± 6.6	0.0 ± 0.0

Mean ± SD.
Mean of individual litter values.
1): Number in 20 sections/part/dam.

maternal sinusoids and a decrease in the cellular density of trophoblastic septa[18]. Therefore, the present study revealed that the small placenta in the testosterone-induced rat model of PCOS occurred only at the end of gestation. Histopathologically, it was assumed that the testosterone-induced small placenta was associated with the developmental inhibition of the fetal part of the placentas from GD 17 onwards. In addition, no increased apoptosis or decreased cell proliferation was elicited during gestation.

Testosterone is an anabolic hormone, and an increased testosterone concentration in the fetal environment can be expected to facilitate growth rather than have a negative impact on fetal growth[19]. In addition, maternal testosterone does not cross the placenta to directly suppress fetal growth[8]. However, elevated maternal testosterone is known to induce IUGR and low-birth-weight offspring in rats[7], humans[17], and sheep[20]. IUGR in PCOS is thought to be induced by an abnormal utero-placental blood flow[9, 21] and placental hypoxia[13, 22]. In the testosterone-induced rat model of PCOS[9, 23], elevated maternal testosterone elicits pregnancy-induced hypertension and a reduced utero-placental blood flow due to the inhibition of the endothelium-dependent relaxation pathway involving nitric oxide production in blood vessels with the renin-angiotensin system[24]. In addition, testosterone induces the downregulation of genes related to vascular development and angiogenesis and reduces the growth of the utero-placental vascular tree that evolves in the placenta[9]. In the present study, IUGR was detected only on GD 21 but not on GD 15 or 17, where it did not occur in the small placenta. Histopathologically, there were no obvious changes in vascular development in the maternal part of the placenta during the experimental period. On the other hand, judging by the histological morphology in the labyrinth zone, an utero-placental blood flow in the small placenta on GD 21 was considered to be reduced compared with normal placenta. Therefore, it was supposed that IUGR in the testosterone-induced rat model of PCOS was attributable to insufficient blood supply for rapid fetal development from GD 17 onwards, as a consequence of the narrowing of maternal sinusoids in the labyrinth zone. However, it was not possible from this study to determine whether the morphological changes in the labyrinth zone associated with the developmental inhibition of the placenta were due to a direct effect of testosterone and/or a secondary effect of the reduced utero-placental blood flow.

In normal human placental development, endovascular trophoblasts invade into the spiral arteries, penetrate, and replace their endothelium. This morphological change, the so-called "endothelial replacement", occurs in the first or early second trimester of gestation[25, 26]. In pregnant women with PCOS, elevated maternal testosterone impairs this trophoblast invasion into spiral arteries in early pregnancy and leads to an inadequate spiral artery remodeling, resulting in increased vascular resistance of utero-placental circulation and a reduced utero-placental blood flow[27, 28]. In normal rat placental development, endovascular trophoblasts invade the spiral arteries from GD 13 or 14 onwards[29], replace endothelium, and lead to sink into the vessel wall on GD 21[30]. In addition, interstitial trophoblasts invade the metrial gland and replace degenerated u-NK cells in perivascular regions. In the present study, it was revealed that testosterone did not inhibit the endovascular trophoblast invasion into the spiral arteries. Rather, the number of spiral arteries with the endothelial trophoblast-invasion increased on GD 15 in the TP-treated group. However, this change was thought to be unrelated to the small placenta and IUGR on GD 21, because there were no differences in the number of spiral arteries with the endothelial trophoblast-invasion on GD 17 in both groups. Thus, the effects on a reduced utero-placental blood flow in the testosterone-induced rat model of PCOS was considered to have no relationship to the inhibition of the endovascular trophoblast invasion into the spiral arteries, unlike PCOS in humans.

In conclusion, IUGR and small placentas were observed only at the end of gestation in the testosterone-induced rat model of PCOS. The small placentas resulted from the thickening of trophoblast septa and the narrowing of maternal sinusoids. It was assumed that the histological morphology in placentas in the testosterone-induced rat model of PCOS was induced in association with the developmental inhibition of the fetal part of the placentas from GD 17 onwards.

Disclosure of Potential Conflicts of Interest: The authors declare no conflict of interest.

Acknowledgement: The authors would like to thank Ms. Yukiko Sudo, Ms. Hiromi Asako, Mr. Atsushi Funakoshi, Ms. Kaori Maejima, Mr. Makoto Tsuchiya, and Mr. Yoshinori Tanaka for their excellent technical assistance.

References

1. Salamalekis E, Bakas P, Vitoratos N, Eleptheriadis M, and Creatsas G. Androgen levels in the third trimester of pregnancy in patients with preeclampsia. Eur J Obstet Gynecol Reprod Biol. **126**: 16–19. 2006. [Medline] [CrossRef]
2. Carlsen SM, Jacobsen G, and Romundstad P. Maternal testosterone levels during pregnancy are associated with offspring size at birth. Eur J Endocrinol. **155**: 365–370. 2006. [Medline] [CrossRef]
3. Boomsma CM, Eijkemans MJ, Hughes EG, Visser GH, Fauser BC, and Macklon NS. A meta-analysis of pregnancy outcomes in women with polycystic ovary syndrome. Hum Reprod Update. **12**: 673–683. 2006. [Medline] [CrossRef]
4. Qin JZ, Pang LH, Li MJ, Fan XJ, Huang RD, and Chen HY. Obstetric complications in women with polycystic ovary syndrome: a systematic review and meta-analysis. Reprod Biol Endocrinol. **11**: 56–70. 2013. [Medline] [CrossRef]
5. Melo AS, Vieira CS, Barbieri MA, Rosa-E-Silva AC, Silva AA, Cardoso VC, Reis RM, Ferriani RA, Silva-de-Sá MF, and Bettiol H. High prevalence of polycystic ovary syndrome in women born small for gestational age. Hum Reprod. **25**: 2124–2131. 2010. [Medline] [CrossRef]
6. Wolf CJ, Hotchkiss A, Ostby JS, LeBlanc GA, and Gray LE

Jr. Effects of prenatal testosterone propionate on the sexual development of male and female rats: a dose-response study. Toxicol Sci. **65**: 71–86. 2002. [Medline] [CrossRef]
7. Sun M, Maliqueo M, Benrick A, Johansson J, Shao R, Hou L, Jansson T, Wu X, and Stener-Victorin E. Maternal androgen excess reduces placental and fetal weights, increases placental steroidogenesis, and leads to long-term health effects in their female offspring. Am J Physiol Endocrinol Metab. **303**: E1373–E1385. 2012. [Medline] [CrossRef]
8. Sathishkumar K, Elkins R, Chinnathambi V, Gao H, Hankins GD, and Yallampalli C. Prenatal testosterone-induced fetal growth restriction is associated with down-regulation of rat placental amino acid transport. Reprod Biol Endocrinol. **9**: 110–122. 2011. [Medline] [CrossRef]
9. Gopalakrishnan K, Mishra JS, Chinnathambi V, Vincent KL, Patrikeev I, Motamedi M, Saade GR, Hankins GD, and Sathishkumar K. Elevated testosterone reduces uterine blood flow, spiral artery elongation, and placental oxygenation in pregnant rats. Hypertension. **67**: 630–639. 2016. [Medline] [CrossRef]
10. Huang J, Zhou S, Ping J, Pan X, Liang G, Xu D, Kou H, Bao C, and Wang H. Role of p53-dependent placental apoptosis in the reproductive and developmental toxicities of caffeine in rodents. Clin Exp Pharmacol Physiol. **39**: 357–363. 2012. [Medline] [CrossRef]
11. Moroki T, Matsuo S, Hatakeyama H, Hayashi S, Matsumoto I, Suzuki S, Kotera T, Kumagai K, and Ozaki K. Databases for technical aspects of immunohistochemistry: 2021 update. J Toxicol Pathol. **34**: 161–180. 2021. [Medline] [CrossRef]
12. Palomba S, Russo T, Falbo A, Di Cello A, Tolino A, Tucci L, La Sala GB, and Zullo F. Macroscopic and microscopic findings of the placenta in women with polycystic ovary syndrome. Hum Reprod. **28**: 2838–2847. 2013. [Medline] [CrossRef]
13. Koster MP, de Wilde MA, Veltman-Verhulst SM, Houben ML, Nikkels PGJ, van Rijn BB, and Fauser BCJM. Placental characteristics in women with polycystic ovary syndrome. Hum Reprod. **30**: 2829–2837. 2015. [Medline]
14. Pan T, He G, Chen M, Bao C, Chen Y, Liu G, Zhou M, Li S, Xu W, and Liu X. Abnormal CYP11A1 gene expression induces excessive autophagy, contributing to the pathogenesis of preeclampsia. Oncotarget. **8**: 89824–89836. 2017. [Medline] [CrossRef]
15. Veiga-Lopez A, Steckler TL, Abbott DH, Welch KB, MohanKumar PS, Phillips DJ, Refsal K, and Padmanabhan V. Developmental programming: impact of excess prenatal testosterone on intrauterine fetal endocrine milieu and growth in sheep. Biol Reprod. **84**: 87–96. 2011. [Medline] [CrossRef]
16. Ling S, Dai A, Williams MR, Myles K, Dilley RJ, Komesaroff PA, and Sudhir K. Testosterone (T) enhances apoptosis-related damage in human vascular endothelial cells. Endocrinology. **143**: 1119–1125. 2002. [Medline] [CrossRef]
17. Kumar S, Gordon GH, Abbott DH, and Mishra JS. Androgens in maternal vascular and placental function: implications for preeclampsia pathogenesis. Reproduction. **156**: R155–R167. 2018. [Medline] [CrossRef]
18. Furukawa S, Tsuji N, and Sugiyama A. Morphology and physiology of rat placenta for toxicological evaluation. J Toxicol Pathol. **32**: 1–17. 2019. [Medline] [CrossRef]
19. Slob AK, and Van der Werff Ten Bosch JJ. Sex differences in body growth in the rat. Physiol Behav. **14**: 353–361. 1975. [Medline] [CrossRef]
20. Beckett EM, Astapova O, Steckler TL, Veiga-Lopez A, and Padmanabhan V. Developmental programing: impact of testosterone on placental differentiation. Reproduction. **148**: 199–209. 2014. [Medline] [CrossRef]
21. Maliqueo M, Echiburú B, and Crisosto N. Sex steroids modulate uterine-placental vasculature: implications for obstetrics and neonatal outcomes. Front Physiol. **7**: 152–159. 2016. [Medline] [CrossRef]
22. Kelley AS, Puttabyatappa M, Ciarelli JN, Zeng L, Smith YR, Lieberman R, Pennathur S, and Padmanabhan V. Prenatal testosterone excess disrupts placental function in a sheep model of polycystic ovary syndrome. Endocrinology. **160**: 2663–2672. 2019. [Medline] [CrossRef]
23. Chinnathambi V, Blesson CS, Vincent KL, Saade GR, Hankins GD, Yallampalli C, and Sathishkumar K. Elevated testosterone levels during rat pregnancy cause hypersensitivity to angiotensin II and attenuation of endothelium-dependent vasodilation in uterine arteries. Hypertension. **64**: 405–414. 2014. [Medline] [CrossRef]
24. Chinnathambi V, Balakrishnan M, Ramadoss J, Yallampalli C, and Sathishkumar K. Testosterone alters maternal vascular adaptations: role of the endothelial NO system. Hypertension. **61**: 647–654. 2013. [Medline] [CrossRef]
25. Kaufmann P, Black S, and Huppertz B. Endovascular trophoblast invasion: implications for the pathogenesis of intrauterine growth retardation and preeclampsia. Biol Reprod. **69**: 1–7. 2003. [Medline] [CrossRef]
26. Pijnenborg R, Vercruysse L, Hassens M, and Van Assche FA. Trophoblast invasion in pre-eclampsia and other pregnancy disorders. In: Pre-eclampsia. Etiology and Clinical Practice, 1st ed. F Lyall, and M Belfort (eds). Cambridge University Press, Cambridge. 3–19. 2007.
27. Palomba S, Russo T, Falbo A, Di Cello A, Amendola G, Mazza R, Tolino A, Zullo F, Tucci L, and La Sala GB. Decidual endovascular trophoblast invasion in women with polycystic ovary syndrome: an experimental case-control study. J Clin Endocrinol Metab. **97**: 2441–2449. 2012. [Medline] [CrossRef]
28. Prefumo F, Sebire NJ, and Thilaganathan B. Decreased endovascular trophoblast invasion in first trimester pregnancies with high-resistance uterine artery Doppler indices. Hum Reprod. **19**: 206–209. 2004. [Medline] [CrossRef]
29. Caluwaerts S, Vercruysse L, Luyten C, and Pijnenborg R. Endovascular trophoblast invasion and associated structural changes in uterine spiral arteries of the pregnant rat. Placenta. **26**: 574–584. 2005. [Medline] [CrossRef]
30. Pijnenborg R, and Vercruysse L. Animal models of deep trophoblast invasion. In: Placental Bed Disorders, 1st ed. R Pijnenborg, I Brosens, and R Romero (eds). Cambridge University Press, Cambridge. 127–140. 2010.